



EDGEWOOD

CHEMICAL BIOLOGICAL CENTER

U.S. ARMY RESEARCH, DEVELOPMENT AND ENGINEERING COMMAND

ECBC-CR-091

EVALUATION OF 5-CM AGENT FATE WIND TUNNEL VELOCITY PROFILES

James E. Danberg



SCIENCE APPLICATIONS
INTERNATIONAL CORPORATION
San Diego, CA 92121

September 2007

Approved for public release;
distribution is unlimited.



20071015181

ABERDEEN PROVING GROUND, MD 21010-5424

Disclaimer

The findings in this report are not to be construed as an official Department of the Army position unless so designated by other authorizing documents.

REPORT DOCUMENTATION PAGE

Form Approved
OMB No. 0704-0188

Public reporting burden for this collection of information is estimated to average 1 hour per response, including the time for reviewing instructions, searching existing data sources, gathering and maintaining the data needed, and completing and reviewing this collection of information. Send comments regarding this burden estimate or any other aspect of this collection of information, including suggestions for reducing this burden to Department of Defense, Washington Headquarters Services, Directorate for Information Operations and Reports (0704-0188), 1215 Jefferson Davis Highway, Suite 1204, Arlington, VA 22202-4302. Respondents should be aware that notwithstanding any other provision of law, no person shall be subject to any penalty for failing to comply with a collection of information if it does not display a currently valid OMB control number. **PLEASE DO NOT RETURN YOUR FORM TO THE ABOVE ADDRESS.**

1. REPORT DATE (DD-MM-YYYY)

XX-09-2007

2. REPORT TYPE

Final

3. DATES COVERED (From - To)

May 2006 - Oct 2006

4. TITLE AND SUBTITLE

Evaluation of 5-cm Agent Fate Wind Tunnel Velocity Profiles

5a. CONTRACT NUMBER

DAAD13-03-D-0017

5b. GRANT NUMBER

5c. PROGRAM ELEMENT NUMBER

SAIC Agreement No. 669338

5d. PROJECT NUMBER

5e. TASK NUMBER

5f. WORK UNIT NUMBER

6. AUTHOR(S)

Danberg, James E.

7. PERFORMING ORGANIZATION NAME(S) AND ADDRESS(ES)

SAIC, 10260 Campus Pt. Drive, San Diego, CA 92121

8. PERFORMING ORGANIZATION
REPORT NUMBER

ECBC-CR-091

9. SPONSORING / MONITORING AGENCY NAME(S) AND ADDRESS(ES)

DIR, ECBC, ATTN: AMSRD-ECB-RT-TD, APG, MD 21010-5424

10. SPONSOR/MONITOR'S
ACRONYM(S)

11. SPONSOR/MONITOR'S REPORT
NUMBER(S)

12. DISTRIBUTION / AVAILABILITY STATEMENT

Approved for public release; distribution is unlimited.

13. SUPPLEMENTARY NOTES

COTR: Dan Weber, AMSRD-ECB-RT-TD, (410) 436-2158

14. ABSTRACT

Velocity profiles measured in 5-cm Agent Fate wind tunnels have been evaluated for conformance to specified profiles. These facilities are used to determine evaporation and desorption rates of chemical warfare agents (CWA) from various surface materials. The specified profiles represent an atmospheric boundary layer for velocity conditions of 6, 3, and 0.5 m/s at a height of 2 m. The 5-cm tunnels are designed to duplicate the part of this profile closest to the surface to provide realistic conditions for agent volatilization. The friction velocity that characterizes the flow in the wall layer of turbulent boundary layers was obtained for each profile from the semi-logarithmic region of the velocity distribution. Results show that the average friction velocities at the two highest velocities are slightly below that of the predetermined values by 7.5 and 8.4%, respectively. This difference corresponds to a systematic error in agent evaporation rate of 4-5%. Other characteristics of the velocity distributions (e.g., the intercept in the semi-logarithmic coordinates) varied significantly from the zero pressure gradient turbulent boundary layer. The low velocity measurements were found to be essentially laminar with turbulence intensity measurements confirming this laminar character.

15. SUBJECT TERMS

CWA
Law of the Wall
Turbulent Boundary Layer
Friction velocity

Velocity distribution
Laminar Boundary Layer

Zero pressure gradient
Turbulence intensity

16. SECURITY CLASSIFICATION OF:

a. REPORT

U

b. ABSTRACT

U

c. THIS PAGE

U

17. LIMITATION
OF ABSTRACT

UL

18. NUMBER
OF PAGES

42

19a. NAME OF RESPONSIBLE
PERSON

Sandra J. Johnson

19b. TELEPHONE NUMBER (include
area code)
(410) 436-2914

15. SUBJECT TERMS (Continued)

Evaporation

Agent fate

Wind tunnel

Velocity profile

PREFACE

The work described in this report was authorized under Contract No. DAAD13-03-D-0017. The work was started in May 2006 and completed in October 2006.

The text of this contractor report is published as received and was not edited by the Technical Releases Office, U.S. Army Edgewood Chemical Biological Center.

The use of either trade or manufacturers' names in this report does not constitute an official endorsement of any commercial products. This report may not be cited for purposes of advertisement.

This report has been approved for public release. Registered users should request additional copies from the Defense Technical Information Center; unregistered users should direct such requests to the National Technical Information Service.

Blank

CONTENTS

1.	INTRODUCTION	7
1.1	Overall Objective of the Fate Wind Tunnel Program.....	7
1.2	Theoretical Analysis of the Evaporation Rate	8
2.	APPROACH	9
2.1	Semi-Empirical Theory of Equilibrium Turbulent Boundary Layer, Log-Law and Law-of-the-Wall Variables	9
2.2	The Use of the Log-Law to Predict the Friction Velocity and Shear Stress.....	9
2.3	The Law-of-the-Wall Region.....	10
2.4	An Empirical Description of the Wall Region.....	11
2.5	Least Square Data Reduction.....	11
2.6	Predefined Operational Velocity Profile.....	11
3.	RESULTS	14
3.1	Law-of-the-Wall Parameters Determined by Least Square	14
3.2	Horizontal (T3L) and Vertical (T3B) Inlet Tunnels	14
3.3	Profiles in Physical Semi-Log Coordinates	18
3.4	Profiles in Physical Coordinates	19
3.5	Low Speed Data.....	23
3.6	Turbulence Intensity Measurements	25
4.	CONCLUSIONS.....	29
5.	RECOMMENDATIONS	31
6.	NOMENCLATURE	39
	LITERATURE CITED	41

FIGURES

1: Operational Non-Dimensional Velocity Profile	13
2: Log-Law Slope (Run T3L-HA7-8).....	15
3: T3B Non-Dimensional Velocity Profile vs Operational Profile.....	16
4: T3L Non-Dimensional Velocity Profile vs Operational Profile.....	17
5: Semi-Logarithmic T3B Profiles vs Operational Profile	19
6: T3L-MA1-2 Compared with Operational Profile.....	20
7: T3B-MA1-3 Compared to Operational Profile.....	21
8: T3L-HA7-8 Compared to Operational Profile.....	21
9: T3B-HA1-3 Compared to Operational Profile	22
10: T3L-LA13-14 Profile Compared to Operational Profile	24
11: Low Velocity Law of the Wall	25
12: Comparison of Turbulence Intensity with and without Screens.....	26
13: Effect of Velocity on Turbulence Intensity	27

TABLES

1: Design Operational Conditions at 35 °C	12
2: Comparison of Friction Velocity for Two Representative Profiles.....	15
3: Friction Velocity Data for All Profiles	18
4: Velocities at 1 and 2 cm.....	22
5: Low Speed Friction Velocity Compared with Operational Data.....	23
6: Reynolds Number, Shape Factor and C_f	28

EVALUATION OF 5-CM AGENT FATE WIND TUNNEL VELOCITY PROFILES

1. INTRODUCTION

The objective of this report is to provide an independent evaluation of the degree to which the experimental velocity profile measurements in the 5-cm ECBC wind tunnels agree with the predetermined theoretical profile (designated the Operational Profile.)

1.1 Overall Objective of the Fate Wind Tunnel Program.

The ultimate applications of the 5-cm tunnel results are summarized in the following quotes.

“The general goal is to develop an integrated and validated atmospheric transport modeling capability for chemical and biological agent releases”¹.

“Transport and diffusion models are powerful tools for assessing the consequences resulting from routine industrial emissions, accidental releases of hazardous materials, and dissemination of chemical and biological warfare agents”².

The 5-cm wind tunnel program^{3,4,5} contribution to the broader program is to provide a facility for the measurement of secondary evaporation (i.e., evaporation of the agent from natural and man-made surfaces after ground impact as contrasted with primary air borne drops.) of hazardous agents. Because hazardous materials are involved, there are several size limitations on each tunnel to carry out all testing within the confines of a standard chemical fume hood. The mass loss from a single drop is measured as a function time as a first step to considering the more complicate situation of the interaction of multiple drops. The drops to be tested in the 5-cm tunnels are very small of the order of 9 ml or smaller and when deposited on an impervious wall material such as glass the protuberance height is less than 0.5 mm. The facility is designed to accommodate other kinds of surfaces that might involve sorption of the drop or even a chemical reaction with the surface material.

One of the elements in designing transport and diffusion models is the question of the atmospheric convection effect on the evaporation rate. The evaporation rate depends on the concentration distribution in the vicinity of the drop surface and the concentration distribution is affected by the velocity distribution. The problem of the diffusion of the evaporated vapor into the more general atmospheric flow field cannot be considered in small-scale facilities such as this. However, the results are made useful to the more general problem by selecting operational conditions for the atmospheric flow consisting of three velocity conditions at a fixed elevation of 2 m. It is then assumed that the flow field between the 2 m height and the surface is that of a zero pressure gradient equilibrium turbulent boundary layer. Thus, the tunnel condition is to simulate the last 2 cm of this boundary layer. To accomplish this, use is made of roughness elements (i.e.,

turbulence generators) to artificially produce the velocity distribution specified by the operational conditions.

1.2 Theoretical Analysis of the Evaporation Rate.

To provide guidance on the relationship between the velocity field and the other parameters that affect the evaporation rate, a simple two-dimensional problem of evaporation into a laminar Couette flow was investigated⁶. This represents the sessile drop condition present with HD on glass during the 5-cm Wind Tunnel validation tests. The method employed was an integral technique. A similar approach to the sessile droplet evaporation was used by Baines and James⁷ and obtained almost identical results but their solution used a similarity technique. The result, in its most general form of Sherwood number, Reynolds number and Schmidt number is:

$$Sh_d = 0.825 Re_d^{2/3} Sc^{1/3} \quad (1)$$

The non-dimensional Sherwood number and Reynolds numbers are defined in terms of Couette flow velocity field, i.e., the friction velocity, u_τ , the stream-wise dimension of the drop, d , (in this instance, the drop diameter) and the properties of air and the evaporated vapor. In physical variable terms the evaporation rate \dot{M} (Kg/s) becomes

$$\dot{M} \propto \left[d^{5/3} \right] \left[\left(\frac{\nu}{D} \right)^{1/3} \frac{Dc_w}{\nu^{2/3}} \right] \left[u_\tau^{2/3} \right] \quad (2)$$

The droplet diameter could also be interpreted in terms of the initial drop volume as $d = Q^{1/3}$. The central term is a combination of fluid properties, D , the diffusivity of vapor in air, ν , the kinematic viscosity of air and c_w the saturation concentration of the evaporated vapor at the surface of the drop. All these factors are a function of the temperature of the system. The comparison of this relationship with experimental data⁸ shows that the best-fit exponent of the Reynolds number is closer to 1/2 than 2/3 and that the constant of 0.825 in Equation (1) over predicts the magnitude of the evaporation by 13%. The inability to accurately predict the magnitude is explained in part by the two-dimensional approximation that does not account for the lateral diffusion and possible effect of the lateral turbulent diffusion in this near wall layer. Nevertheless, the analysis suggests that for small sessile droplets, the evaporation rate is directly related to the friction velocity. Thus, evaluation of the 5-cm tunnel profiles can be judged in terms of the success in duplicating u_τ .

2. APPROACH

2.1 Semi-Empirical Theory of Equilibrium Turbulent Boundary Layer, Log-Law and Law-of-the-Wall Variables.

It is generally established that fully developed equilibrium turbulent layers (boundary layers or internal flows) include a region identified as the Logarithmic-layer^{9,10}. That is, the velocity profile can be represented by an equation of the form, where u equals the velocity parallel to the surface and y the normal to the surface.)

$$u \propto \ln(y) \quad (3)$$

In the wall region it has been found experimentally that Equation (3) can be written as:

$$\frac{u}{u_\tau} = \frac{1}{\kappa} \ln\left(\frac{u_\tau y}{\nu}\right) + C \quad (4)$$

Where ν is the kinematic viscosity, κ and C are constants, and u_τ is the friction velocity:

$$u_\tau = \sqrt{\frac{\tau_w}{\rho}} \quad (5)$$

(Where τ_w is the stress acting on the surface and ρ is the air density)

The quantity $\kappa \cong 0.4$ is the von Karman Universal Constant of Turbulence and is observed to be a useful constant in describing turbulent wall flows. The value of this constant was initially derived from the pipe flow data of Nikuradse (1930) and in the literature values of 0.40-0.42 are often cited for equilibrium zero pressure gradient turbulent boundary layers.

2.2 The Use of the Log-Law to Predict the Friction Velocity and Shear Stress.

One of the consequences of the Log-Law is that the slope of the velocity versus $\ln(y)$ profile is directly related to the friction velocity, that is:

$$\frac{du}{d \ln(y)} = \frac{u_\tau}{\kappa} \quad (6)$$

Thus, if κ is a given constant, Equation (6) provides a simple way of determining the wall friction velocity and shear stress. In general there are two related practical problems in carrying out this procedure. First, in most boundary layers the Log-Law region is relatively small seldom more than 10% of the total boundary layer thickness and it is located near the wall where measurements are most difficult. The second problem is determining where the Log-Law starts and ends so that the slope is not corrupted by

deviations from this condition. Visual observation of a straight line in the semi-logarithmic plot of the data is not reliable for small deviation and in the presence of random scatter in the measurements.

A linear least square technique is used to fit $u = a + b \ln(y)$ where $u_\tau = \kappa b$. Once u_τ has been determined then the constant is calculated using Equation (4):

$$C = \frac{a}{u_\tau} - \frac{1}{\kappa} \ln\left(\frac{u_\tau}{v}\right) \quad (7)$$

2.3 The Law-of-the-Wall Region.

The standard picture of a boundary layer is of a sublayer adjacent to the smooth wall with a transition or buffer layer between it and the fully turbulent layer described by Equation (4). The question becomes how to describe the departure from the Log-Law into the transition region. The van Driest damping in the Prandtl mixing length theory as described by Cebeci and Smith¹¹ (Chapter 4) provides an approximation. In this approach the shear stress is taken to be the sum of the laminar stress and the turbulent stress in the following form.

$$\tau = \mu \frac{\partial u}{\partial y} + \rho \ell^2 \left(\frac{\partial u}{\partial y} \right)^2 \quad (8)$$

The ℓ is a mixing length, which was originally defined by Prandtl as κy was modified by van Driest to account for a damping effect on the turbulence as the surface is approached.

$$\ell_{vD} = \kappa y \left(1 - e^{-\frac{y^+}{A^+}} \right) \quad (9)$$

If we make the assumption that the shear is constant throughout the viscous sub-layer at the surface value, then using the law-of-the-wall velocity u^+ and y^+ variables, Equations (8) and (9) can be put in the form.

$$\frac{du^+}{dy^+} = \frac{-1 + \sqrt{1 + 4\ell^{+2}}}{2\ell^{+2}} \quad (10)$$

As the mixing length goes to zero near the wall the non-dimensional velocity slope goes to 1 corresponding to the slope in the sublayer. At large values of y relative to A^+ , the slope approaches the Log-Law limit of $1/\kappa y^+$. It is a simple matter to numerically

integrate Equation (10) from the boundary condition of $u^+ = 0$ at $y^+ = 0$ to any large value of y^+ arbitrarily close to the Log-Law. A value of $A^+ = 27.5$ in Equations (9) and (10) results in the estimation of the fully turbulent non-dimensional profile with an intercept C of 5.5.

2.4 An Empirical Description of the Wall Region.

An alternate empirical description of the wall region is derived by assuming a constant velocity slope in the near wall region $y^+ \leq 5$ followed by a buffer or transition region where $5 \geq y^+ \leq 30$ based on a Log-Law equation but defining the slope and intercept using the $u^+ = y^+ = 5$ point in the sublayer and a second point on the Log-Law at $y^+ = 30$. This results in the following transition equation for $C = 5.5$.

$$u^+ = 5.02 \ln(y^+) - 3.09 \quad (11)$$

If the intercept, C , in the Log-Law remains a parameter but all the y^+ locations remain the same a generalized transition equation becomes.

$$u^+ = (1.96 + 0.56C) \ln(y^+) + (1.85 - 0.90C) \quad (12)$$

Above the transition region the Log-Law is assumed to complete this empirical description of the wall region.

2.5 Least Square Data Reduction.

A FORTRAN program was developed to take three or more data points from the measured profile and to perform a linear least squares fit to u versus $\ln(y)$ to compute the slope, and assuming $\kappa = 0.4$, to determine the most likely value of u_τ and the intercept C . The initial points were selected by trial and error but usually excluded the 2 or 3 points nearest the wall and where the outer points deviated from the linear. Most of the primary profile measurements were made at the center of the test section (Position A) and were repeated up to three times and these runs were grouped together. Uncertainty statistics for the fit were also obtained. In addition, the viscous layer thickness as defined by the maximum in velocity was provided by a quadratic fit to the measurements in the vicinity of the maximum velocity. The numerical data were transferred to a plotting routine where the least square fits were compared with the data.

2.6 Predefined Operational Velocity Profile.

Agent Fate model developers¹² define a set of design objectives for the 5-cm tunnels consisting of three velocities 0.5, 3.0, 6.0 m/s at a height of 2 m above the ground. It is then assumed that the smooth wall equilibrium turbulent boundary layer existed within the 2 m. Thus, Equation (4) was used to determine the velocity profile below 2 m (taking $\kappa = 0.4$ and

$C = 5.5$) and since the friction velocity, u_τ , is the only unknown in Equation (4) it is easily determined.

It was also specified that the wind tunnel reproduce that part of the defined profile consistent with the size of the facility. Since the tunnels are very nearly 5 cm in test section height and because of symmetry, at most, only half that width is available it was, therefore, the design goal to duplicate the last 2 cm of the 2 m layers described above. Based on the friction velocities the velocities at 0.02 m were calculated and listed in Table 1.

Table 1: Design Operational Conditions at 35 °C		
Velocity (m/s) @ 2 m	u_τ , Friction Velocity (m/s)	Velocity (m/s) @ 0.02 m
0.5	0.020	0.26
3.0	0.1038	1.79
6.0	0.1966	3.70

A TSI Hotwire Anemometry system was used to measure the velocity profiles and the turbulence intensity distribution in the 5-cm tunnels. At the low speeds involved in the boundary layer, wall interference effects limit the proximity to the tunnel wall where the hotwire provides unreliable data, that minimum height is 0.127 cm. These critical points are shown in the following “law-of-the-wall” coordinates in Figure 1. In the low speed case the range of the measurements are within the transition region and do not extend into the log-law region. Whereas the high-speed case is entirely within the log-law and the mid speed is predicted to have a substantial range in the log-law but with the lower points extending into the transition region.

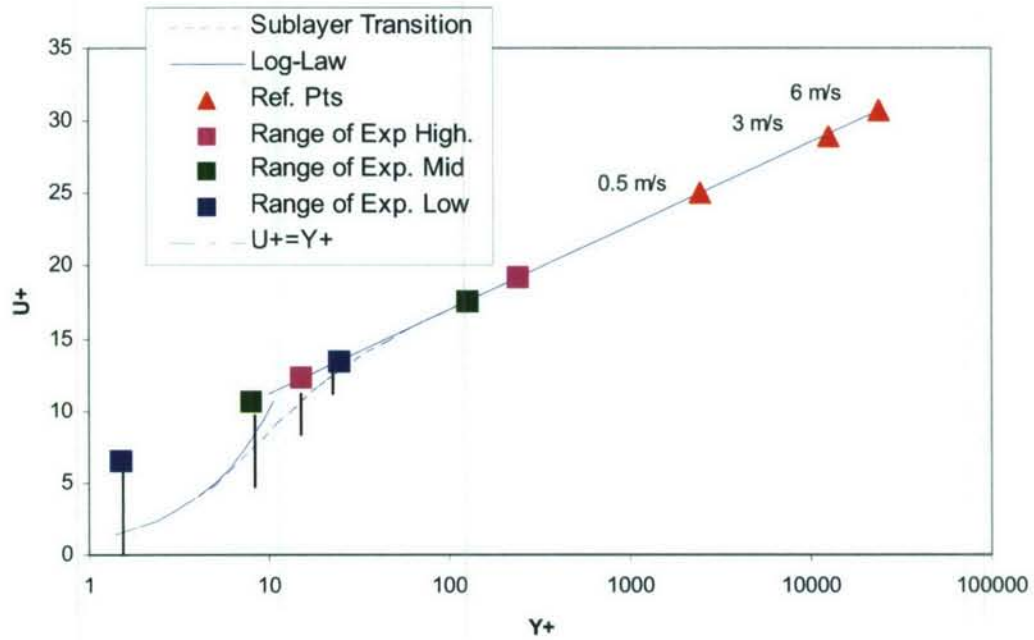


Figure 1: Operational Non-Dimensional Velocity Profile

Test Conditions and Notation

The experimental data accumulated in the 5-cm tunnels involved a range of test conditions. First there were 12 different tunnels constructed and for the purposes of this report they are designated T3A through T3L although only a sample of these have been considered here. Tests were performed at three velocity conditions denoted as High, Mid and Low for the 2 cm equivalent of the 6, 3, 0.5 m/s operational velocities, respectively. Measurements were made at four locations surrounding the primary station designated station A where the focus will be in the following. Two tunnel configurations were developed one with a horizontal inlet that required a portion of the inlet to breach the fume hood and a second model with a vertical inlet, which is entirely accommodated by the hood. A concern is the effect the inlet orientation has on the experimental profiles. The latter tunnel also included a fine mesh screen at the exit of the turning vane section (i.e., entrance to the fetch. Details of the configuration are discussed in Weber et al¹³.

3. RESULTS

3.1 Law-of-the-Wall Parameters Determined by Least Square.

The objective is to evaluate the comparison of the 5-cm tunnel data with the operational profile. This can be accomplished graphically in three ways; first by plotting the data in Law of the Wall coordinates; second by using physical variables in a semi-logarithmic plot; third using physical variables in a linear plot of velocity versus distance from the wall. Examples of all three forms are used in the following. However, the difficulty of evaluating the degree of agreement is in establishing a quantitative criterion.

For the small sessile drops being considered here, the friction velocity, u_{τ} , is the most important convection parameter in determining the evaporation rate. The friction velocity defines the near-wall velocity distribution for a smooth wall. As we have seen, the specification of the velocity at 2 m along with the assumed profile form (Log-Law) defines the friction velocity. Other assumptions regarding the atmospheric boundary layer might be made resulting in a different relationship between the reference velocity and the friction velocity but the evaporation rate would still be characterized by u_{τ} .

Even in the case of a rough wall the friction velocity will still help define the near wall velocity distribution in conjunction with some measure of the roughness height. Thus, in comparing the 5-cm wind tunnel measurements with the last 2 cm of the operational Profile, the starting point is the friction velocity.

3.2 Horizontal (T3L) and Vertical (T3B) Inlet Tunnels.

Two series of profile measurements are considered representing the horizontal inlet configuration with no inlet screen (T3B) and the vertical inlet configuration with the standard 44% porosity screen (T3L). The friction velocity was determined from the slope of u versus $\ln(y)$ assuming the von Karman universal constant of turbulence $\kappa=0.4$. A linear least squares technique was used with 3-7 data points identified as falling in the linear range. Figure 2 illustrates the quality of the fit. The numerical results for the two series (multiple profiles at same condition are analyzed together) are given in Table 2.

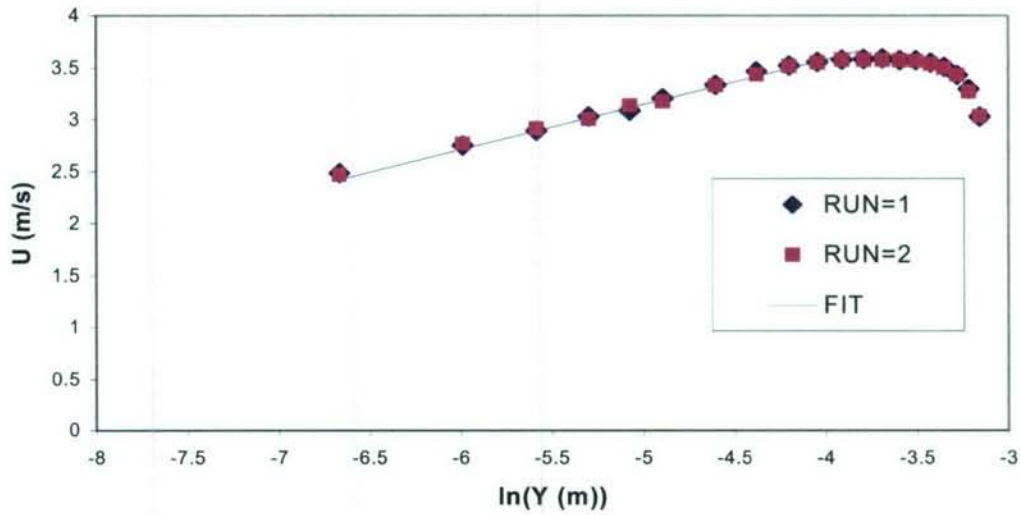


Figure 2: Log-Law Slope (Run T3L-HA7-8)

Table 2: Comparison of Friction Velocity for Two Representative Profiles								
Operational			T3B-A1-3			T3L-A1-3		
	u_τ (m/s)	C	u_τ (m/s)	$2\sigma u_\tau$ %	C	u_τ (m/s)	$2\sigma u_\tau$ %	C
High	0.1966	5.5	0.1595	23	9.2	0.1743	8.3	7.2
Mid	0.1038	5.5	0.0883	17	7.9	0.0785	7.5	10.2

This table's rows designated High and Mid correspond to the 2 m velocities of 6 and 3 m/s. The u_τ determined from the measurements are consistently less than the operational profile by an average of 14%. Relative consistency is shown because the high velocity results remain roughly twice the mid speed case in agreement with the operational results. The change from horizontal to vertical inlet shows no consistent trend. A measure of the uncertainty of the evaluation of u_τ is the two-sigma value obtained by a propagation of error technique during the least square analysis. The T3B profiles were one of the first measured and have considerably more scatter than the T3L data. In addition to the experience accumulated, the T3L data were obtained after installation of the screens, which seems to have a positive effect on the scatter but not on the basic slope and intercept results.

Figures 3 and 4 present the 0 to 2 cm profiles in non-dimensional form (u^+, y^+) using the velocity scale u_τ and the length scale v/u_τ and compared with the operational profile.

Consistent with the table's data, the measurements are considerably higher than the operational curve; however, the slopes are in general agreement.

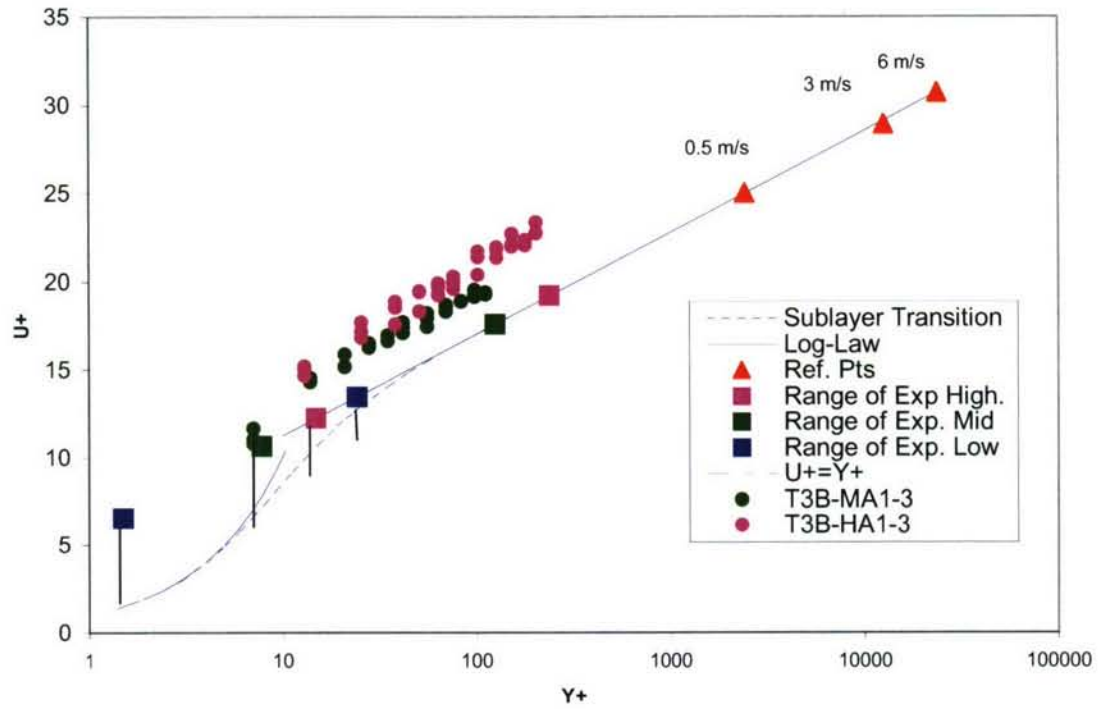


Figure 3: T3B Non-Dimensional Velocity Profile vs Operational Profile

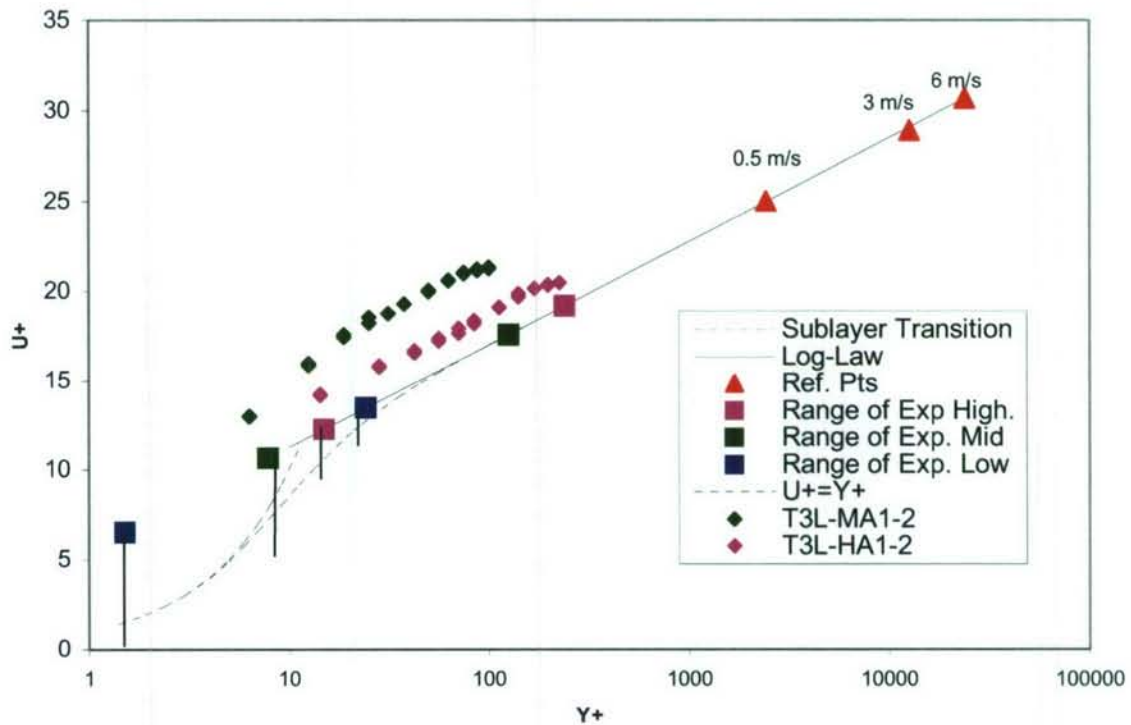


Figure 4: T3L Non-Dimensional Velocity Profile vs Operational Profile

The shift in the measurements relative to the operational curve are reflected in the intercept C obtained from the least square fit. Since there is no trend with velocity in these data, an overall average of $C=8.5 \pm 1.0$ describes the data whereas the assumed value for the operational profile is $C=5.5$. The cause of this modification of the profile from the normal is not clear but one possibility is a departure from two-dimensionality because of the small scale of the facility with sidewall interference. The fact that the inlet flow moves through a 90-degree bend and over unsymmetrical tripping roughness only 5 test section heights upstream of the primary measuring station is suspected also as a factor.

Table 3: Friction Velocity Data for All Profiles				
RUNS	u_{τ} m/s	$2\sigma u_{\tau}$ %	C	COMMENT
T3B-HA1-3	0.160	23	9.2	Horiz. Inlet, No Screens
T3F-HA9-10	0.202	6.0	4.5	Horiz. Inlet, No Screens
T3G-HA3-4	0.189	3.7	5.2	Horiz. Inlet, No Screens
T3F-HA11-12	0.188	6.0	5.8	Horiz. Inlet, No Screens
AVERAGE	0.184		6.2	
T3L-HA1-2	0.174	8.3	7.2	Vert. Inlet, 44% Porosity Screens
T3EYE-HA3-4	0.201	4.3	4.7	Vert. Inlet, 44% Porosity Screens
T3K-HA8-9	0.158	6.4	9.4	Vert. Inlet, 44% Porosity Screens
AVERAGE	0.178		6.9	
T3G-MA1-2	0.096	5.4	6.1	Horiz. Inlet, No Screens
T3F-MA5-6	0.103	9.3	5.2	Horiz. Inlet, No Screens
T3F-MA7-8	0.108	7.6	4.3	Horiz. Inlet, No Screens
T3B-MA1-3	0.088	17	7.9	Horiz. Inlet, No Screens
T3F2-MA2	0.102	13.1	5.4	Horiz. Inlet, No Screens
AVERAGE	0.100		5.6	
T3K-MA6-7	0.099	6.8	5.8	Vert. Inlet, 44% Porosity Screens
T3L-MA1-2	0.078	8.3	10.2	Vert. Inlet, 44% Porosity Screens
T3EYE-MA1-2	0.099	5.6	6.08	Vert. Inlet, 44% Porosity Screens
AVERAGE	0.092		7.4	

Not all the profiles investigated show such a large value for the intercept C. A more complete picture can be gained from Table 3 where friction velocity and C are presented for fifteen profiles. All of these profiles were measured at the primary measuring station (position A) and are for the standard operating temperature of 35 ° C. The average of all the runs is $C=6.6$ and $u_{\tau}=0.180$ and 0.096 for the high and mid velocities, respectively.

Using these results it is possible to work back to obtain the velocity at 2 m for the average measured profile, i.e., $u_{2m} = 5.7$ and 2.9 m/s, which differ only slightly from the operational values.

3.3 Profiles in Physical Semi-Log Coordinates.

Figure 5 is an alternate presentation of the data in physical variables but in a semi-logarithmic format. The experimental data are plotted with a corresponding curve based on the operational profile. In this case the operational profile is computed based on the mixing length analysis. The $u^+ = y^+$ line is based on the operational friction velocity (which is higher than the least squares value.)

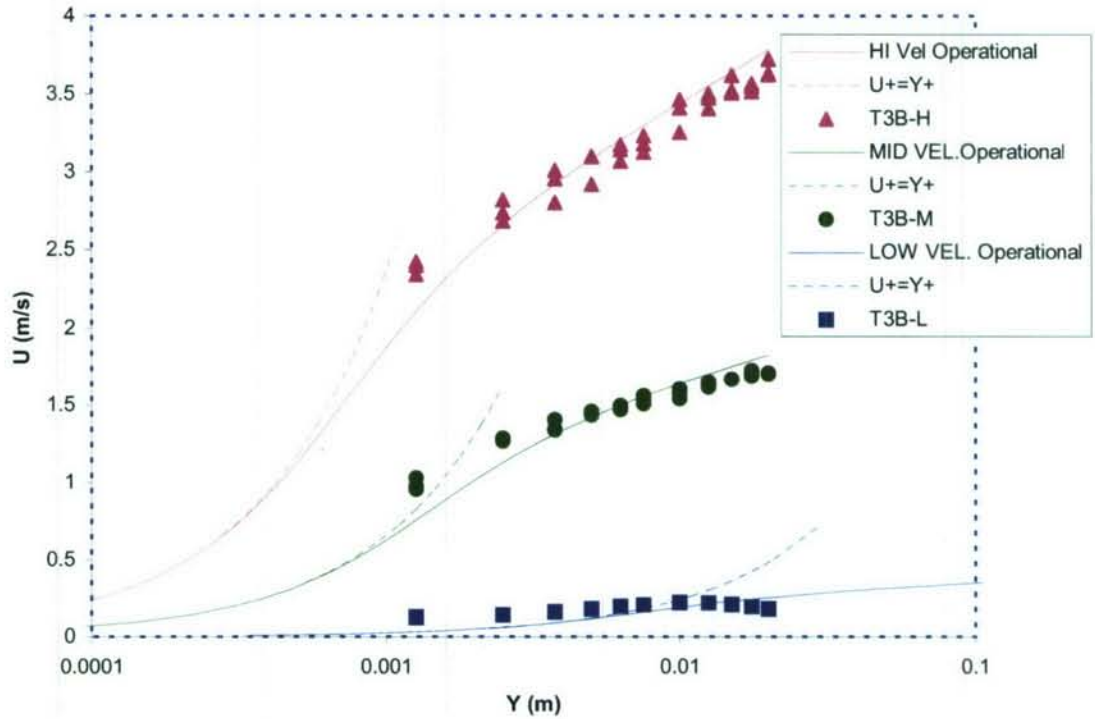


Figure 5: Semi-Logarithmic T3B Profiles vs Operational Profile

This figure emphasizes that the primary effect in reducing the 2 m velocity in half is to reduce the entire profile by a corresponding amount. The operational profile is based on the Van Driest damping mixing length of Equations (9) and (10) and a constant total shear stress. It provides a continuous distribution of velocity through the transition layer to the laminar sublayer. Although it may not be accurate in detail it is expected to provide a reasonable description of these layers for the operational profile but not when the intercept C becomes large. One characteristic is that the experimental data nearest the wall tends to deviate significantly above the theoretical curve. In some cases the last point exceeds the $u^+ = y^+$ line, which implies that that the local total stress exceeds the wall stress that is generally considered inconsistent with wall generated viscous friction. Thus, there is doubt about the accuracy of the data closest to the wall.

3.4 Profiles in Physical Coordinates.

Figures 6 through 9 show the experimental data in linear physical coordinates compared with the operational profile and the least squares fit. In all these plots, the operational and the fit profiles have the same components.

Sublayer: $y^+ < 5$, $u = u_\tau y^+$

Buffer layer: $5 \leq y^+ < 30$, $u = u_\tau ((1.96 + 0.56C)\ln(y^+) + (1.85 - 0.90C))$

Fully turbulent: $y^+ \geq 30$, $u = 2.5\ln(y^+) + C$

Where: $y = vy^+/u_\tau$ and u_τ and C are the operational profile values or for the fit profile the values for that set of runs.

The least squares fit better represents the 2 cm data except for the points closest to the wall. The operational profile tends to pass through the data near the wall but then it diverges with distance. A slightly steeper slope for the operational profile in the sublayer and in the fully turbulent region is consistent with the friction velocity values. These figures show that the objective of creating the last 2 cm approaching the ground of a theoretical distribution is reasonably well approximated. As expected, the operational and least square fit distributions deviate from the data in the wake region near the centerline of the 5 cm Wind Tunnel.

The buffer layer equations under-estimates the local measurements in this region for the operational and “least squares” fit profile. This is less noticeable at the higher velocity in part because fewer points are in the buffer region. Also, the interaction between the hot wire anemometer and the wall tends to increase the measured velocity, which would be more important at the lower velocity

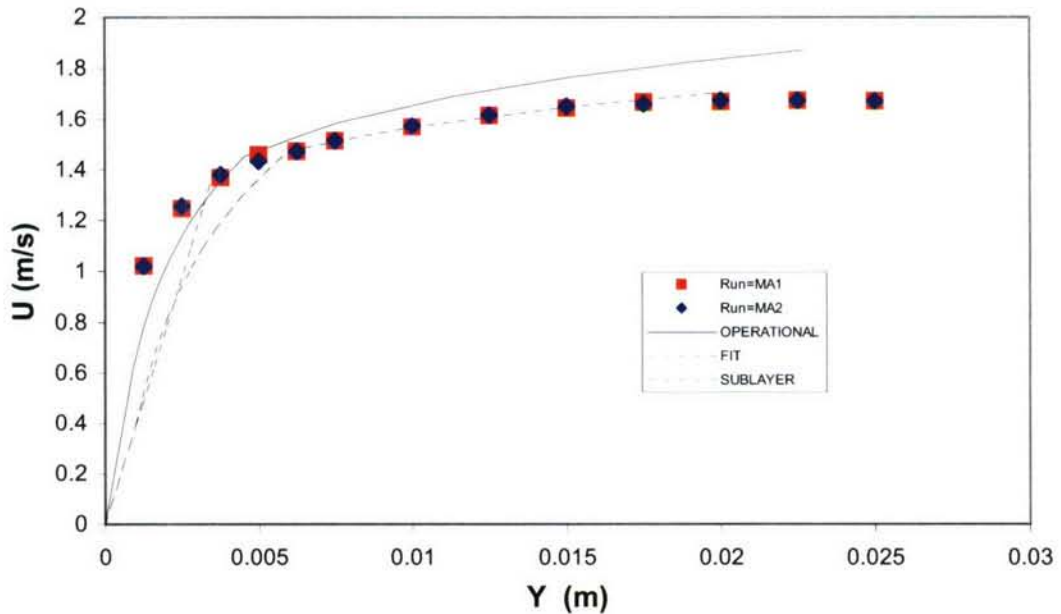


Figure 6: T3L-MA1-2 Compared with Operational Profile

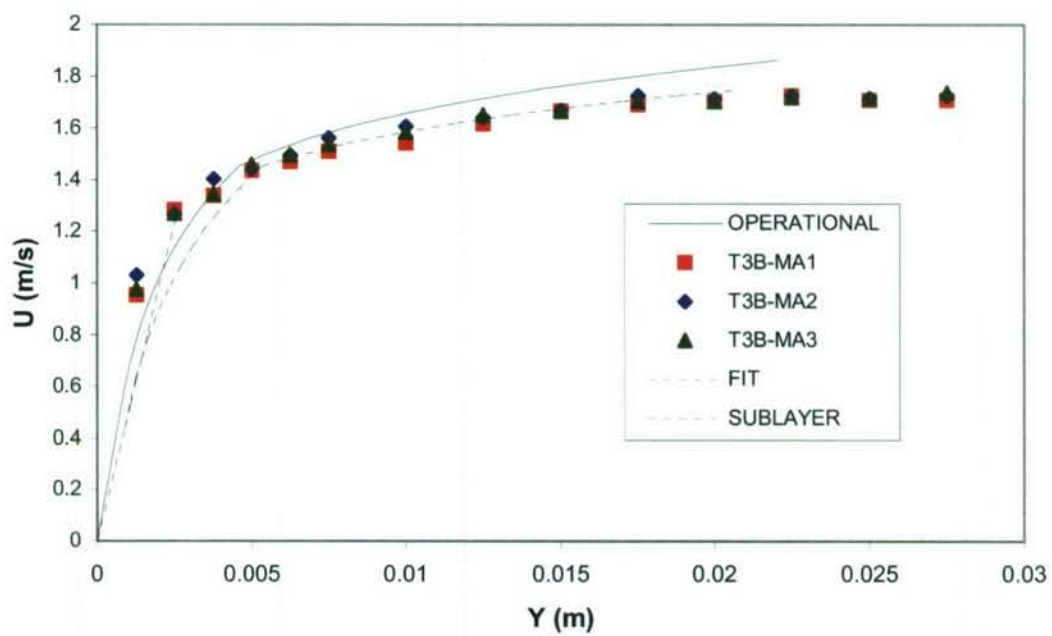


Figure 7: T3B-MA1-3 Compared to Operational Profile

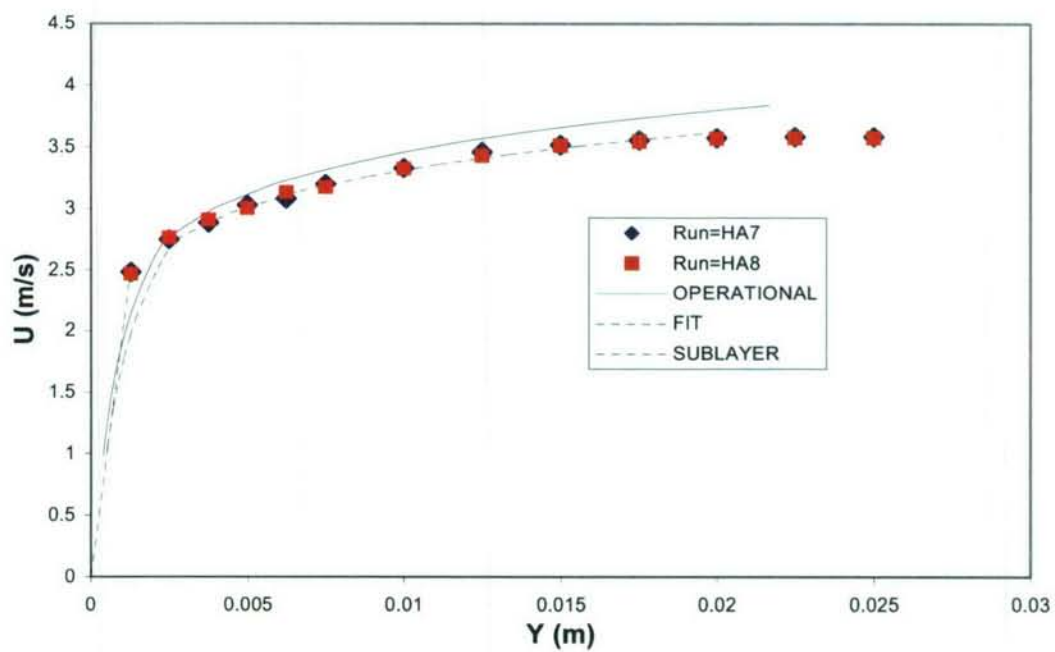


Figure 8: T3L-HA7-8 Compared to Operational Profile

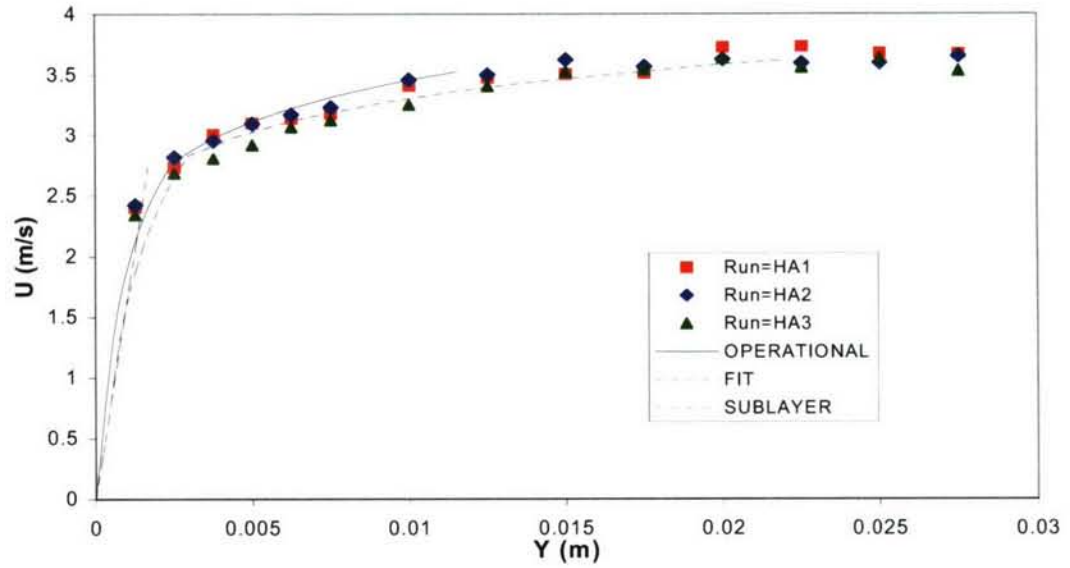


Figure 9: T3B-HA1-3 Compared to Operational Profile

The velocity at 1 or 2 cm were the desired matching points for the tunnel profiles, and Table 4 shows how well this velocity condition was achieved for four runs.

Table 4: Velocities at 1 and 2 cm				
	Operational Profile (m/s)	Measured Profile (m/s)	Difference %	LS Fit Profile (m/s)
Velocities at 1 cm				
T3B-HA1-3	3.45	3.37	-2.2	3.32
T3L-HA7-8	3.45	3.33	-3.6	3.30
T3B-MA1-3	1.66	1.58	-4.7	1.58
T3L-MA1-2	1.66	1.57	-5.2	1.59
Velocities at 2 cm				
T3B-HA1-3	3.69	3.66	-0.8	3.57
T3L-HA7-8	3.70	3.57	-3.6	3.62
T3B-MA1-3	1.80	1.71	-5.0	1.74
T3L-MA1-2	1.79	1.67	-6.7	1.71

Thus, the goal of matching the operational 1 and 2 cm velocities were missed by falling only about 5-6% low. The least square fit $u_{2\text{cm}}$ agrees closely with the experimental data, which again shows that the data and fit diverge somewhat from the operational Profile.

3.5 Low Speed Data.

The low velocity data would be expected to fall, for the most part, in the transition or buffer region between the laminar sublayer and the fully turbulent or the log-law region. Thus, the analysis of the low velocity profile assuming a semi-logarithmic region is not applicable as it is for the higher two velocities. The measurements extended sufficiently near the wall so that the velocity gradient at the wall is obtained by extrapolation and thus the wall shear stress and the friction velocity can be determined.

The existing computer code was modified to skip the log-law analysis and perform the extrapolation in the following form

$$u = Ay + By^2 + Cy^3 \quad (13)$$

In this form the boundary condition $u \rightarrow 0$ as $y \rightarrow 0$ is automatically satisfied. To actually carryout the fitting of the data to determine the coefficients, the data were put into the form of u/y vs. y or

$$\frac{u}{y} = A + By + Cy^2 \quad (14)$$

The same least square subroutine was employed to evaluate the coefficients. Trials showed that the data point closest to the wall had to be excluded to obtain anything like a monotonic fit and then only a limited number of profile data points (≤ 4) could be used. The shape of the measured profile is more complicated than can be described by such a simple formula without introducing inflections in the fitted curve.

The resulting station "A" T3L, T3B data are given in Table 5. Note that $u_\tau = \sqrt{\nu A}$.

Table 5: Low Speed Friction Velocity Compared with Operational Data				
Tunnel	From Data			Operational
	u_τ (m/s)	δ (m)	u_δ (m/s)	u_τ (m/s)
T3L	0.0396	0.011	0.221	0.02
T3B	0.0390	0.010	0.216	0.02

The ability of the quadratic fit to describe the near wall points for the T3L case is shown in Figure 10. The operational predicted slope and profile are indicated by a dashed line in the figure. The operational profile is calculated for 35 C , $u_\tau=0.02$ m/s and:

$$\begin{aligned}
u^+ &= y^+, \text{ for } y^+ < 5 \\
u^+ &= 5.02 \ln(y^+) - 3.09, \text{ for } 5 \leq y^+ \leq 30 \\
u^+ &= 2.5 \ln(y^+) + 5.5, \text{ for } y^+ \geq 30
\end{aligned} \tag{15}$$

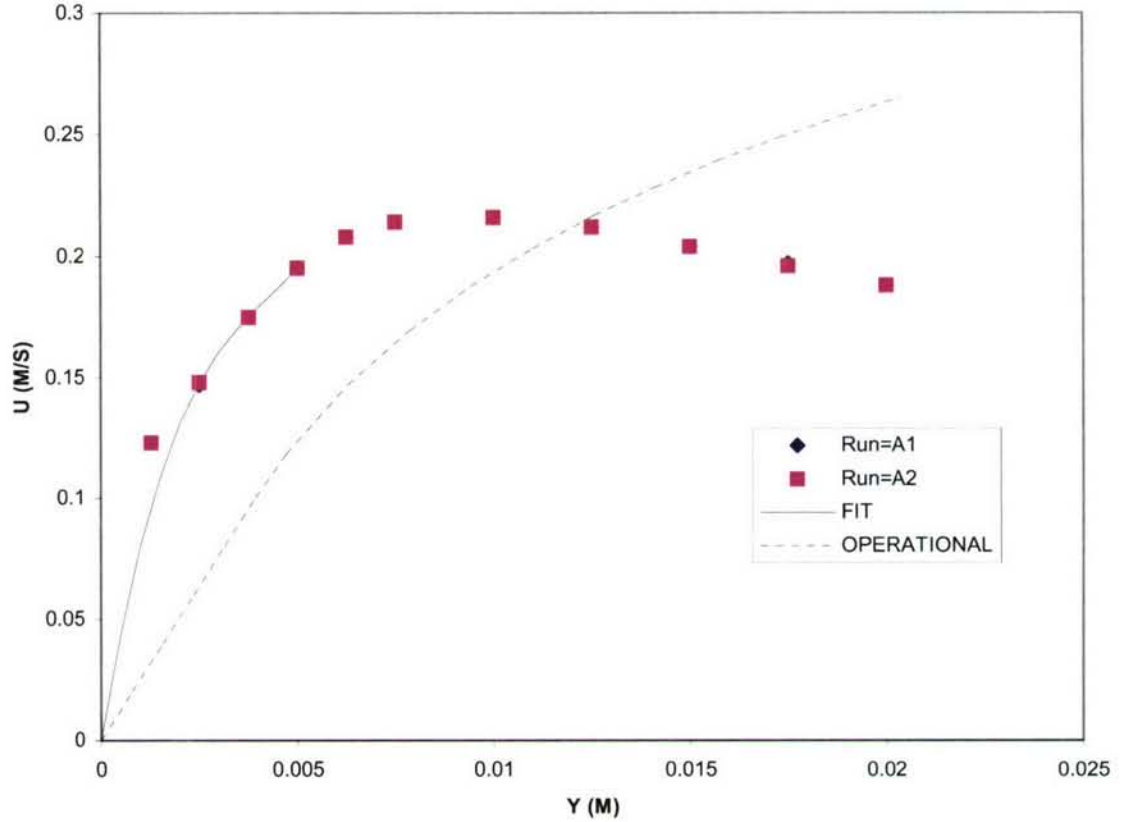


Figure 10: T3L-LA13-14 Profile Compared to Operational Profile

The friction velocity calculated by the above procedure is a factor of two larger than the operational profile prediction. It is difficult to see how the existing data could be extrapolated to the wall with a wall slope as small as required (by a factor of 4.) Linearly extrapolating the next to the last data point gives a value of $u_\tau \cong 0.03$ that is still 50% larger than the operational prediction. It is possible that the data at this low velocity could be contaminated by wall interference. Assuming the u_τ obtained in this way allows the profile to be plotted in the law-of-the-wall coordinates as shown Figure 11. In these coordinates the data fall well below the sublayer $u^+ = y^+$ line and the empirical buffer layer line.

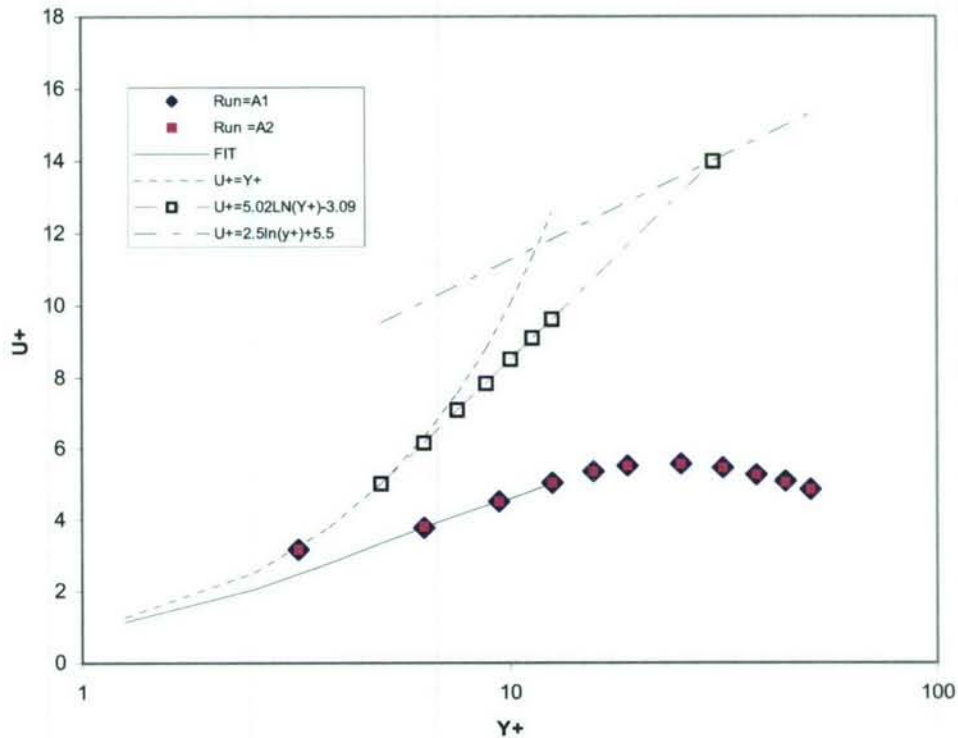


Figure 11: Low Velocity Law of the Wall

The deviation from the buffer layer distribution in the law-of-the-wall coordinates does not correspond to the desired turbulent profile. It appears appropriate to consider the low speed data to be a laminar boundary layer with some imposed turbulence from the tripping elements. The friction velocity correlates a laminar boundary layer wall region just as well as for the turbulent boundary layer. Thus, u_τ represents the characteristic convection velocity for the laminar evaporation just as well as for the turbulent flow. For the same u_τ a laminar boundary layer may be expected to produce the same evaporation rate as long as the concentration distribution in the vicinity of the drop is not affected by the turbulence away from the fluid surface.

For the estimated friction velocity of 0.04 the operational turbulent profile 2-m velocity is 1.07 m/s rather than the target of 0.5 m/s.

3.6 Turbulence Intensity Measurements.

As part of the hot wire data acquisition, turbulent intensity measurements were obtained in the form of root-mean-square stream-wise fluctuations. Consult Weber¹³ et al for details of the technique. The measured turbulence intensities are in the form of u'/u where u is the local mean velocity. To emphasize the sublayer, the data are re-normalized by the friction velocity rather than the local velocity. This is appropriate because the

interest here is with the wall layer and the outer edge of the wind tunnel boundary layer is unrelated to the operational profile.

The turbulent intensity data were converted using $u'^+ = \frac{u'}{u} u^+$. The results for selected profiles are compared to the results cited by Klewicki¹⁴ and by the results of measurements of Klebanoff as cited in Hinze¹⁵. The 5-cm tunnel turbulence intensity falls considerably lower than that of Klebanoff's data and only in the high velocity cases (T3B) do they approach that of the data given by Klewicki as can be seen in Figure 12. The variation of the velocity in the data is also indicative of the variation of the Reynolds number. The T3B data refer to horizontal inlet tunnels without screens. Note that T3K-MA5 and -MA6 are with inlet screens of 61 and 44% porosity, respectively. As might be expected the turbulence intensity decreases with decreasing porosity.

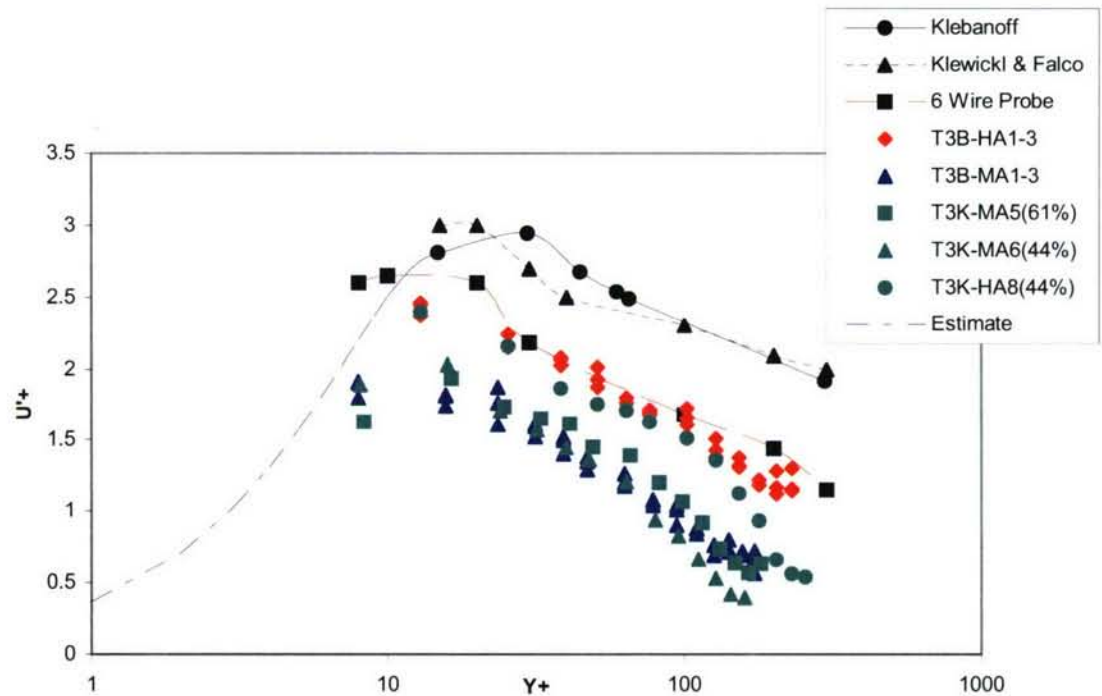


Figure 12: Comparison of Turbulence Intensity with and without Screens

Figure 13 provides examples of the wall layer turbulence level for all three velocities. The maximum of the low velocity intensity data normalized by the friction velocity is more than a factor of 100 less than the mid and high velocity cases for most of the runs. This provides additional evidence that the low velocity data should be considered laminar and treated differently than the higher velocity data.

* The Klebanoff and Klewicki data were scaled from graphs and intended to show only general magnitude and trends.

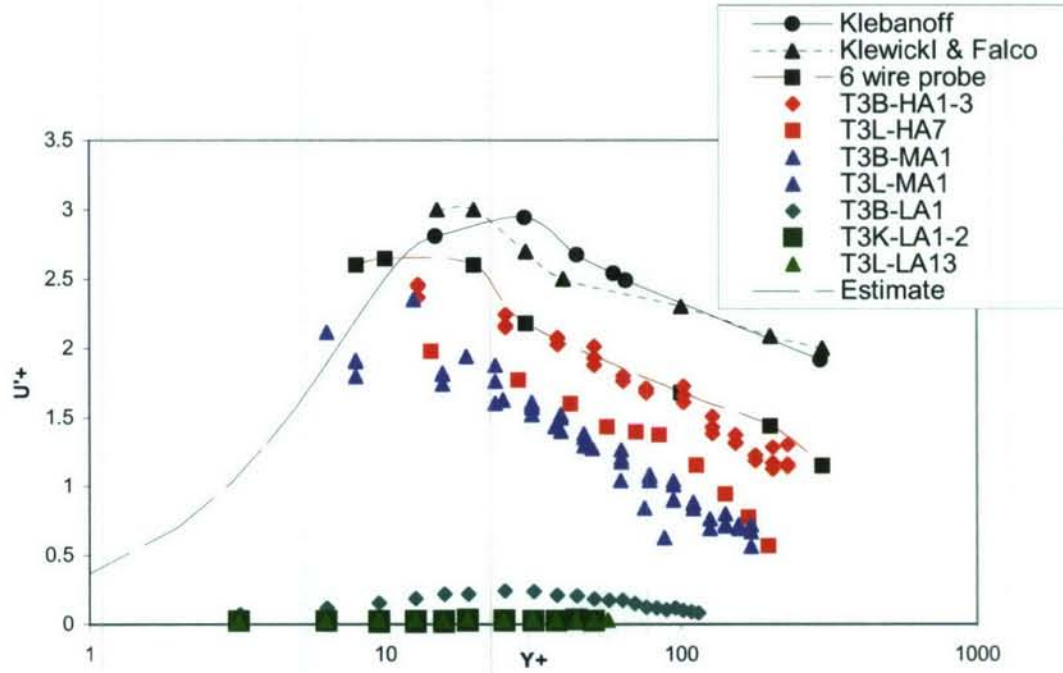


Figure 13: Effect of Velocity on Turbulence Intensity

The velocity levels for the wind tunnel data correspond directly to the Reynolds number of the measurements. To quantify the Reynolds number for the experiments the integral boundary layer parameters of momentum, Θ , and displacement, δ^* , thickness were computed numerically from the velocity profile data. The definition of these quantities is given by the following formulas:

$$\Theta = \int_0^{\delta} \frac{u}{u_{\delta}} \left[1 - \frac{u}{u_{\delta}} \right] dy \quad (16)$$

$$\delta^* = \int_0^{\delta} \left[1 - \frac{u}{u_{\delta}} \right] dy \quad (17)$$

Either the Momentum or displacement thickness may be used as the length scale in the Reynolds number. Both are provided in Table 6 along with the shape factor and the skin friction coefficient based on the friction velocity. Klebanoff's experiment corresponds to a displacement thickness Reynolds number of 11,200. A laminar Blasius profile has a constant shape factor of 2.59. On the other hand, an equilibrium zero pressure gradient turbulent boundary layer has a shape factor that is a function of Reynolds number. At $Re_{\delta} = 305$, $H = 1.49$, and at $Re_{\delta} = 2480$, H decreases slightly to 1.36^{16} .

Table 6: Reynolds Number, Shape Factor and C_f				
TUNNEL	Re_δ	H	$C_f = 2 \left[\frac{u_\tau}{u_\delta} \right]^2$	Re_{δ^*}
T3B-HA1-3	491	1.51	0.0010	741
T3K-HA8-9	740	1.41	0.0009	1043
T3L-HA7-8	459	1.53	0.0012	702
T3B-MA1-3	185	1.66	0.0013	307
T3L-MA1-2	153	1.71	0.0011	262
T3K-MA5 (61% porosity)	297	1.61	0.0058	478
T3K-MA6-7 (44% porosity)	356	1.50	0.0016	534
T3B-LA1-2	61	1.61	0.0161	98
T3K-LA10-11 (44% porosity)	12	2.09	0.0174	25
T3L-LA13-14	13	2.12	0.0163	28

The displacement thickness Reynolds number has the significance of defining the minimum critical condition for amplification of disturbances in a laminar (Blasius) boundary layer. The neutral stability curves have been rigorously defined by various investigators as cited by Schlichting⁸ and White¹⁵ (pgs 400-403.) The critical value of Re_{δ^*} is 520.

Examination of Table 6 shows that the high velocity cases are above the critical Reynolds number, while the mid speed range is somewhat below critical. The low speed cases are all less than a fifth of the stability limit, which suggests that the effect of the turbulence generators is strongly damped. Thus, even if the atmospheric boundary layer of 2 m at the 0.5 m/s speed is turbulent, it is not possible to create a turbulent boundary layer (even artificially) at the corresponding speed in a 5-cm facility.

4. CONCLUSIONS

The objective is to compare and evaluate the degree to which the measured 5-cm tunnel velocity profiles agree with the predetermined turbulent operational profile at three velocity conditions. The problem is how to formulate a criterion to quantify the comparison. It seems important in formulating such a criterion to study the evaporation mechanism, which is the ultimate purpose for creating these facilities. A tentative two-dimensional model has been suggested based on the assumption that the evaporating sessile droplet is sufficiently small that the concentration of its vapor is confined to the immediate vicinity of the droplet in the near wall layer. Thus, a model employing a Couette flow can be used to show that the characteristic convection velocity is the friction velocity. To the extent this model is valid, the operational profile and the experimental data can be compared in terms of how well the friction velocities agree. The slope of the turbulent semi-logarithmic profile is used to determine the experimental friction velocities from the measurements.

At the high and mid velocity conditions, corresponding to the operational profiles at 6 and 3 m/s, respectively, the friction velocities are 0.180, 0.096 m/s with an average intercept C of 6.6, which are different from the operational values of 0.1966, 0.1038 m/s and C of 5.5. Thus, the experimental friction velocity data are consistently lower by 7.5% and 8.4%, respectively than specified by the reference and the intercept is consistently higher by 18%. The uncertainty in individual tests in terms of two standard deviations in the friction velocity varies considerably with a high of 23% and a low of 4% with an overall average of 8.7%. Thus, the potential uncertainty is of the same order as the deficit in the friction velocity with respect to the operational profile. The evaporation model modified by initial test data predicts the evaporation rate to depend on the friction velocity to the $1/2$ power and thus the uncertainty in rate due to friction velocity could be of the order of 4-5% on average.

The intercept in the Log-Law varies considerably in individual tests from a high of just over 10 to a low in the 4's with an average of 6.6. In principle the intercept is not relevant to the sublayer velocity gradient and friction velocity. However, it is of concern in that it is an indication of the extent of the sublayer and the rapidity of the damping of the turbulence as the wall is approached. In addition it may be an indication of the lack of two-dimensionality of the flow.

The low velocity condition is a special case. Theoretically the operational profile predicts that most of the low speed data to be mostly in the buffer layer and that the semi-logarithmic slope cannot be used to determine the friction velocity. As an alternative the data were extrapolated to the wall and the slope of the resulting curve used to determine the shear stress and friction velocity. The results show the friction velocity to be 0.04 m/s compared to the expected value of 0.02 m/s. The data plotted in law-of-the-wall coordinates show that the experimental data deviate very significantly from that of a turbulent profile suggesting the low speed measurements were essentially laminar.

Examination of the turbulent intensity data confirm that the velocity fluctuation level is substantially lower than observed for the other velocities. It is probably impossible to produce a turbulent boundary layer at such a low velocity in a 5-cm tunnel. The friction velocity of the laminar flow can also be related to hypothetical 2 m turbulent boundary layer at a velocity of about 1 m/s.

5. RECOMMENDATIONS

As a consequence of the various aspects of this study the following eight recommendations have been identified and are suggested for further experimental and analytical investigation. The reasons for and possible approaches to carrying out these recommendations are developed in some detail in the following paragraph.

- 1-Flow symmetry
- 2-Additional velocities both higher & between mid and low
- 3-Drop protuberance
- 4-Multiple Drops
- 5-Roughness
- 6-Thin-film-heat transfer
- 7-Computational program
- 8-Hot Wire measurement of w'

1-Flow Symmetry

An effort should be made to make the flow in the 5-cm tunnels more symmetric or at least to evaluate the effects of improved symmetry. The concern is that the asymmetries, particularly the effect of the turbulence generators acting on just one side of the tunnel induces secondary circulations that detract from the two-dimensionality of the viscous boundary layer at the measuring station. Possibly the lack of symmetry might help explain the high value of the Log-Law intercept observed in the measurements.

2-Additional Velocities

The predetermined operational low velocity condition is inconsistent with a turbulent boundary layer in the 5-cm tunnel because at that velocity the turbulence generators become ineffective. Under the assumption that the atmospheric boundary is turbulent it might be desirable to expand the velocities conditions in the tunnel to find the minimum consistent with turbulence.

3-Drop protuberance

A 9 ml sessile drop of HD on glass presents a 0.5 mm height segment of a sphere protuberance to the flow that has been ignored in the analysis of the evaporation rate in the model proposed⁶. Although the drop is expected to be smooth with a gentle slope (contact angle of about 20°) the height is significant and its effects should be evaluated. A first step might be to make profile measurements above and behind a simulated drop. The presence of protuberances on aerodynamic surfaces is common and must have been addressed experimentally and analytically (although perhaps not at the Reynolds numbers of the 5-cm tunnel); therefore, a literature search is recommended.

4-Multiple Drops

A critical problem in formulating an analysis of the effect of multiple sessile drops on the overall contaminant production is the interaction between the droplets. The greater the separation, longitudinally and laterally, the less the interaction and beyond a certain separation the evaporation rates are completely independent. A study should be made of the suitability of the 5-cm tunnels for the purpose of measuring the effect of separation distance on two drops in tandem.

As guidance in this study use can be made of the 2-D analysis of the evaporation rate. For example if two drops are aligned one behind the other and touching they can be considered as one large drop. The model predicts that the local evaporation rate per unit area, N , is proportional to a function of the x position on the drop.

$$N \propto \left(\frac{x}{d} \right)^{-1/3}$$

Thus, for the front half of a large drop the average evaporation rate, \bar{N}_f , is proportional to the integral over the front half of the drop and similarly the average rate, \bar{N}_r , is the integral over the rear. The predicted ratio is:

$$\frac{\bar{N}_r}{\bar{N}_f} = 0.587$$

But the average evaporation rate is also proportional to the concentration driving potential for evaporation, which in general form is $c_w - c_\delta$. Where c_w is determined by the saturation vapor pressure of the agent. In the case of a single drop evaporating into a stream devoid of any trace of the agent, then the “background” concentration $c_\delta = 0$. If we assume the entire deficit in evaporation rate for the rear drop is due to a background concentration being different from zero, then

$$c_{\delta r} = 0.413c_w$$

This background concentration is presumably a maximum when the two drops are adjacent and it decreases with separation distance as the contaminated plume of agent from the foreword drop spreads and diffuses. The 5-cm tunnel configured for two drops might provide useful data on the effect of separation distance on the evaporation of the downstream drop. Analysis of the effective background concentration may be interpretable in terms of the initial diffusion of the agent from the upstream source.

The ultimate application is to an analytical scheme to estimate the total production from array of drops. Given the delivery mechanism an estimate is made of the distribution of drops and the probability of drops falling with certain proximities and combined with the

information on the decrease in evaporation rates at the appropriate separation distances would finally add up to a prediction of the total output.

5-Roughness

A fully rough surface is characterized by a roughness height, k , where the roughness Reynolds number, $Re_k = u_\tau k / \nu$, is equal or greater than 70. For the high velocity operational profile ($u_\tau = 0.2 \text{ m/s}$) $k = 5.6 \text{ cm}$, which exceeds the capability of a small wind tunnel and represents unrealistic situation except in the case of a rock strewn area. However, the lower limit at which surface roughness begins to produce an effect is $Re_k \approx 4$ or a height of 3 mm. Roughness heights up to 10-15 mm may be feasible in the 5-cm tunnel.

Imagining the sand grain roughness as hemispheres, the spacing between peaks would be twice the height. A 9 ml HD drop spreads out to cover a 6.3 mm circle on a glass surface. Thus, the 9 ml drop might be expected to only partially fill the valleys between the peaks. Whether this would represent an effectively larger evaporating surface needs to be determined.

The effect of roughness on evaporation and heat transfer is different in mechanism from its effect on skin friction because skin friction forces are transmitted to the protuberances by pressures forces, which have no counter part in evaporation and heat transfer. Evaporation mass transfer is analogous to heat transfer; therefore, the heat transfer results are taken as representative of the trend to be expected for evaporation. Taking heat transfer theory (see Kays and Crawford¹ pages 298-301) as a guide to evaporation, a 60% increase in heat transfer was calculated and theory agreed with the data cited for the $Re_k \approx 70$ fully rough case (the momentum thickness Reynolds number for the data was about 10,000, which is 20 times that of the 5-cm tunnel case). If the effect of roughness is linear this suggests a 10% increase in evaporation would be observed in the 5-cm tunnel. There are a number of unknown factors that could affect the magnitude such as non-linearity of the effect and the condition that the drop would fill the valleys to variable depths affecting the exposed droplet surface area.

A practical consideration in providing a fully rough surface in the 5-cm tunnel concerns how much of the tunnel surface needs to be roughened. Thinking of it as a new boundary layer starting at the beginning of the roughness but with a turbulent growth rate. It probably should have roughness as far upstream as possible so that the entire boundary layer at the measuring station is affected by the roughness even though the evaporating agent may only penetrate a fraction of the boundary layer thickness.

6-Thin-film-heat transfer

The suggestion here is to investigate the possibility of using a thin film element on the piston to simulate the evaporation problem with an analogous heat transfer experiment. A thin film heated electrically such that it produces a discontinuous jump in the thermal

boundary condition on the film similar to the jump in concentration at the sessile drop in the evaporation case. Such a simulation has the advantages that the heat transfer rate (analogous to evaporation rate) can be measured from the power supplied to the film.

A possible application of the thin-film technique might be as an instrument to independently measure the wall shear stress or the friction velocity. The conventional assumption of an analogy between the skin friction and heat transfer is not appropriate in the present case because the conventional analogy assumes that the thermal boundary layer and the friction boundary layers begin at the same point and develop together. In the present problem the thermal boundary is initiated at the thin film deep within an established viscous layer. If the same theory of evaporation into a Couette flow is adopted for the heat transfer problem identical results are obtained but in different variables, that is:

$$\overline{Nu} = \frac{\overline{q}_w d}{\rho c_p (T_w - T_\delta) \alpha} = 0.794 \left[\frac{u_\tau d}{\nu} \right]^{2/3} Pr^{1/3}$$

Where: \overline{Nu} = Average Nusselt number
 \overline{q}_w = Wall heat flux (W/m²)
 c_p = Specific heat (kJ/Kg · K)
 α = Thermal diffusivity (m²/s)
 T = Temperature (K)
 Pr = Prandtl number = $\frac{c_p \mu}{k} = \frac{\nu}{\alpha}$
 d = Stream-wise dimension of the thin film

Thus, for the Couette problem the heat transfer coefficient, $\overline{q}_w / (T_w - T_\delta)$, is proportional to the friction velocity to the 2/3 power. It would be desirable to have this as an independent measurement; therefore, it would be important to calibrate the thin film independently. Since the above relationship is applicable in a laminar flow as in a wall layer of a turbulent boundary layer (under the limitation that the temperature distribution is limited to the linear sublayer region.) Calibrating the film in a larger facility compared to the 5-cm tunnels would allow a detailed validation of the laminar character and wall shear stress of the calibrating facility even if a direct measurement of the skin friction were not possible.

The disadvantages include the problem of natural convection and density distortion that may limit the range of temperatures. The tunnel could be inverted since it is not tied to a fume hood thereby minimizing the thermal convection effect. A direct comparison with between heat transfer and evaporation rate would be complicated by the fact that the Prandtl number in Air is 0.7 whereas the Schmidt number for HD in air is 2.5.

7-Computational program

A two-dimensional integral analysis of the evaporation rate was briefly described¹ in the report's introduction and the 2-D limitation should be eliminated to better understand the sessile drop evaporation. A computational fluid dynamic analysis of the three dimensional problem is recommended that would provide a sound basis for interpretation of evaporation rate measurements. The equation describing the balance between diffusion and convection of a vapor, in its most general form, can be written as:

$$\frac{\partial c}{\partial t} + u \frac{\partial c}{\partial x} + v \frac{\partial c}{\partial y} + w \frac{\partial c}{\partial z} = \left(\frac{\partial}{\partial x} \left(D_x \frac{\partial c}{\partial x} \right) + \frac{\partial}{\partial y} \left(D_y \frac{\partial c}{\partial y} \right) + \frac{\partial}{\partial z} \left(D_z \frac{\partial c}{\partial z} \right) \right)$$

Where: c =concentration (Kg/m^3)

D =Diffusivity of vapor in air (m^2/s)

In principle this equation could be solved numerically simultaneously with the continuity and momentum equation of fluid mechanics. The first simplification would be to assume steady state and eliminating the first term. Another approximation that is normally made is to neglect the diffusion term in the stream direction under the assumption that the convection is much stronger. Thus, eliminating the first term on the right hand side. Initially constant properties could be assumed so that the diffusivity is independent of direction and can be factor from the right hand side. Initially the flow field over the height of the sessile drop could be neglected so that the mean w velocity can be taken as zero simplifying the convection terms (but the diffusion in the w direction is retained.) Finally an assumption of symmetry means that the numerical grid boundary plane can pass through the stream-wise centerline of the drop and flow field so that symmetry defines conditions on that boundary.

Other boundary conditions required include an upstream velocity profile, which the experimental data from the 5-cm tunnel provides data. The wall boundary conditions of no slip are combined with $c=0$ everywhere on the surface except at the sessile drop where the surface concentration is determined by the known saturation vapor pressure of the agent. The downstream boundary condition is placed sufficiently far from the drop to have no effect on the evaporation. The free-stream boundary is taken as a constant velocity (zero pressure gradient).

As an approximate solution the assumption might be made that the drop is small enough so that the velocity distribution is fixed in the vicinity of drop where the evaporation rate is determined. If the protuberance of the drop is ignored, such an assumption would permit the simplification of $v=w=0$ and that $u=u(y^+)$.

$$u(y^+) \frac{\partial c}{\partial x} = \frac{\partial}{\partial y} \left(D_y \frac{\partial c}{\partial y} \right) + \frac{\partial}{\partial z} \left(D_z \frac{\partial c}{\partial z} \right)$$

This assumption eliminates the need for a separate continuity and momentum equation. Some assumption is required about the diffusivity. The first step might be to just consider the laminar case with $u = u^{+2}/v$ and D a constant at its molecular value. The turbulent diffusivity is considered in item 5.

Creating a three dimensional grid over the drop (that is assumed 2-D on the surface) the problem becomes that of a 3-D concentration boundary layer developing in a fixed velocity distribution. The formulation of the solution algorithm is still formidable.

8-Hot Wire Measurement of w'

As a rather speculative extension of the above computational project, the diffusivity could be considered a combination of molecular diffusivity and turbulent diffusivity. The turbulent diffusivity is a function of the y and z coordinates and is directional since the gradient in concentration exists in both directions. The w' or cross-flow turbulence is known to be different in magnitude and approaches zero at the surface at a slower rate than the component normal to the surface on which existing models are based. The v' component decreases more quickly than either the u' or w' because of the obstructive presence of the surface inhibits the normal velocities. The transverse and longitudinal motions are not restrained as much because they are only affected by viscosity. This is meant to point out that the turbulent diffusivity, D_{tz} , may not be negligible even when the normal (y) component of the turbulent momentum and mass diffusivity can be considered small. This effect may contribute to higher experimental evaporation rates.

Guidance regarding the magnitude of the transverse component of the turbulence could be obtained by measuring the root mean square w' velocity. This could be accomplished by rotating the wire from its normal orientation if this is feasible with the current instrument.

The analytical problem is based on developing a model for the D_{tz} term as it appears in the following relation (N is the local flux of mass per unit area.)

$$N_z = D \frac{\partial c}{\partial z} - \langle c'w' \rangle = (D + D_{tz}) \frac{\partial c}{\partial z}$$

An extensive literature search should attempt to find any similar problems in heat or mass transfer. However, this seems a unique problem, which has some aspects of a three-dimensional flow of agent in an approximately two-dimensional mean flow. The formulation of a turbulent diffusivity would lean on the studies of eddy thermal diffusion. See for example Kays and Crawford¹⁷ and Arpaci and Larsen¹⁸. In their reviews of algebraic models it appears that a simple first order approximation is to assume a turbulent Schmidt ($\cong 0.9$) that relates the eddy diffusivity (D_{tz}) to the eddy viscosity (mixing length theory) and is also a function of the molecular Schmidt number. The unmodified eddy viscosity in the x - y plane is obviously incorrect because it becomes very small in the sublayer where the turbulent contribution in z direction needs to be

calculated. As a preliminary approximation, the ratio of the w' to u' could be used based on the Klebanoff¹⁵ data to scale the x-y eddy viscosity (mixing length theory) to a w' component eddy viscosity. Confidence in using the Klebanoff data would be increased if it is shown that the measured w' and u' components in the 5-cm tunnel are in the same ratio.

Blank

NOMENCLATURE

A	Surface Area of evaporating drop
A^+	Van Driest damping constant
c_f	Skin friction coefficient
c_w	Concentration of vapor at the surface of drop
C	Intercept in Log-Law
d	Diameter of sessile drop
D	Diffusivity of evaporated vapor in air
H	Boundary layer shape factor
ℓ	Mixing length
L	Characteristic length
\dot{M}	Total evaporation rate
N	Evaporation rate per unit area
Q	Volume of drop
Re_d	Reynolds Number = ud/ν
Re_θ	Reynolds Number based on momentum thickness = $u\theta/\nu$
Sc	Schmidt Number = ν/D
Sh_d	Sherwood Number = $Nd/c_w D$
T	Temperature
u	Stream-wise velocity
u^+	Law-of-the-wall velocity coordinate = u/u_τ
u'	Rms stream-wise velocity fluctuation
u_δ	Velocity at edge of the boundary layer
u_τ	Friction velocity = $\sqrt{\nu \left(\frac{\partial u}{\partial y} \right)_w}$
u_δ^+	u_δ/u_τ
y	Coordinate normal to the surface
y^+	Law-of-the-wall coordinate variable = $u_\tau y/\nu$

Greek Symbols

β	Contact angle of sessile drop
θ	Momentum thickness
δ	Boundary layer thickness
δ^*	Displacement thickness
κ	von Karman universal constant of turbulence

μ	Air absolute viscosity
ν	Air kinematic viscosity
ρ	Air density
τ	Shear stress
σ	Standard deviation

LITERATURE CITED

- ¹ Anon., "Survey and Discussion of Models Applicable to the Transport and Fate Thrust Area of the Department of Energy Chemical and Biological Nonproliferation Program," Contributors: Argonne, Lawrence Berkeley, Lawrence Livermore and Los Alamos National Laboratories, September 1997.
- ² Chang, J. C., P. Franzese, K. Chayantrakom, S. R. Hanna, "Evaluations of CALPUFF, HPAC, and VLSTRACK with two Mesoscale Fields Datasets," J. Applied Meteorology, vol. 42, April 2003.
- ³ Weber, D., M. Scudder, C. Moury, K. Park, K. Sumpter, S. Hong, T. D'Onofrio, W. Shuely, M. Miller, R. Nickol, B. King, J. Pence, and D. Durst, "Agent Fate 5-cm Wind Tunnel, Version 3: Design Through Testing," Proceedings of the Joint Service Chemical and Biological Decontamination Conference, November 2005.
- ⁴ Weber, D., M. Scudder, C. Moury, K. Park, K. Sumpter, S. Hong, T. D'Onofrio, W. Shuely, M. Miller, R. Nickol, B. King, J. Pence, and D. Durst, "Agent Fate 5-cm Wind Tunnel: Enhancements, Characterization and Performance," Proceedings of the Conference on Chemical Defense Research, November 2005.
- ⁵ Weber, D. J., Scudder, M. K., Moury, C. S., Molnar, J. W., Shuely, W. J., and Miller, M. C., "Micro Wind Tunnel for Hazardous Chemical Fate Studies," Proposed AIAA paper, 2007.
- ⁶ Danberg, J. E., "Derivation of Evaporation into Couette Flow," Memorandum to ECBC/D. J. Weber, et al, February 2006.
- ⁷ Baines, W. D. and D. F. James, "Evaporation of a Droplet on a Surface," Ind. Eng. Chem. Res., 1994, 33, 411-415.
- ⁸ Danberg, J.E., "Evaporation Rate Data Regression Analysis," Memorandum to ECBC/D. J. Weber, et al, February, 27 2006.
- ⁹ Schlichting, Hermann H., *Boundary-Layer Theory*, 7 Ed., McGraw-Hill, New York, 1979.
- ¹⁰ Coles, D. E. and Hirst, "Proc. Computational Turbulent Boundary-Layers Conference," Vol. II, Department of Mechanical Engineering, Stanford University, Stanford, CA 1968.
- ¹¹ Cebeci, T, and Smith, A. M. O., *Analysis of Turbulent Boundary Layers*, Academic Press, New York, 1974.
- ¹² Hin. A. R. T., "Operational Velocity Profiles Defined," May 2004.

¹³ Weber, D. J., M. K. Scudder, C. S. Moury, W. J. Shuely, J. W. Molnar, M. C. Miller, "Velocity Profile Characterization of 5-cm Fate Wind Tunnel," ECBC-TR-XXX, Edgewood Chemical, Biological Center, Aberdeen Proving Ground, MD, August 2006.

¹⁴ J.C. Klewicki, "On Scaling the Statistical Structure of Turbulent Boundary Layers as it Relates to Agent Fate Issues," Presented at Agent Fate Meeting, undated.

¹⁵ J.O. Hinze, *Turbulence*, McGraw-Hill, 1959, Chap. 7.

¹⁶ White, Frank M., *Viscous Fluid Flow*, McGraw-Hill, New York, 1974.

¹⁷ Kays, W. M., Crawford, M. E., *Convective Heat and Mass Transfer, 3rd Ed.*, McGraw-Hill, New York, 1993.

¹⁸ Arpaci, V. S., and P. S. Larsen, *Convective Heat Transfer*, Prentice Hall, Englewood, NJ, 1984.